WOUND ROLL GENERATED UNSTABLE VIBRATION

by

M. Jorkama[1] and R. von Hertzen[2]
Metso, Paper, Inc.[1]
Helsinki University of Technology[2]
FINLAND

ABSTRACT

Nip contact between the wound roll and the winding drum, rider roll or some other nip roller may cause that the wound roll is deformed into a convex polygon. This deformation process is accompanied with a very strong vibration. The conditions under which this phenomenon occurs depend much on the web properties. For example, in the paper industry some bulky grades with a high layer-to-layer COF are known to be prone to this unstable vibration.

In this paper a simple wind up model, capable of capturing quite comprehensively this phenomenon, is developed. The polygonal pattern formation is modeled as a viscoelastic surface deformation. This results in linear delay differential equations. In order to analyze the stability, the Laplace transformation is performed for the system equations. The inspection of the root locus shows several zones of instability during the winding cycle. In an example, it is shown how the model can be utilized to explain some well-known winder vibration phenomena.

The paper is concluded by stating general beneficial trends for the wind up design and by explaining how to determine the susceptibility of certain webs to unstable vibration by simple laboratory measurements.

NOMENCLATURE

A	system matrix in the Laplace-domain
c_1, c_2	viscous damping coefficients of the winding drum and wound roll, respectively
$e(t)$	deviation of the wound roll's shape from circular evaluated at the nip
$\tilde{e}(t)$	evolution of $e(t)$ during one revolution of the roll
f_1, f_2	first and second harmonic of the wound roll rotation frequency
f_{n1}, f_{n2}	first and second natural frequencies of the system
g_i	diagonal terms of **A** (i = 1,2,3)

k_1	the spring constant of the winding drum
k_2, k_3	spring constants of the delayed and instant recovery elements of the wound roll, respectively
m_0	core mass per unit length
m_1, m_2	the masses of the winding drum and wound roll, respectively
$r(t)$	the deformed radius of the wound roll evaluated at the nip
$r_0(t)$	the undeformed radius of the wound roll evaluated at the nip
r_d	the winding drum radius
R_0	the average of $r_0(t)$ over one roll revolution
s	the Laplace-variable
s_i	the complex roots of equation det**A** = 0 (i = 1,2,3,...)
t	time variable
T	wound roll rotation period
u	deformation of the delayed recovery element
x_1, x_2	the vertical displacements of the winding drum and wound roll, respectively
$\mathbf{X}$	column vector of the state variables in the Laplace-domain
X_1, X_2	Laplace transforms of x_1 and x_2
z	an internal translational degree-of-freedom of the wound roll
Z	Laplace transform of z
w	delay term in the system equations
α	the recovery coefficient of the wound roll
δ	the nip deformation of the wound roll

INTRODUCTION

Vibration is a common problem for two-drum winders running certain paper grades. Although these "vibrating paper" grades are of quite wide variety, some common features of the vibrations can be stated. Firstly, the frequency of the vibration is without exception equal to the wound roll rotation frequency or its integer multiple. Secondly, the paper and roll properties are such that the nip induced wound roll deformations will not fully recover during one roll revolution. As a consequence of these features, the oscillating nip load will cause the wound roll to become deformed into a convex polygon.

The most common self-excited winder vibration categories are:

a) **Vibration during the initial acceleration**

This vibration mode occurs when the winder speed is accelerated from zero speed to full running speed. Typically, this vibration state develops fast at the very end of the acceleration stage. Typical paper grades for which this type of vibration can occur are rough and bulky grades with high COF - such as book papers. However, also some thin, coated and calendered paper grade can vibrate in this mode. Because of this vibration, the roll edges can become uneven and the web can brake. Although not confirmed, the vibration mode relating to this type of vibration is believed to be the one where the wound roll has the largest amplitude (wound roll eigenmode). Since the rolls are still quite light when the vibration takes place, the corresponding natural frequency is quite high, typically 40 – 150 Hz.

b) Roll bouncing, resulting to eccentricity

This is clearly the most serious vibration problem for two-drum winders nowadays. Typically, the grades experiencing this problem are easily wound up to the roll diameter 500 – 700 mm but then, little by little, start increasingly to develop eccentricity. The paper grades with a tendency to the above-mentioned vibration include DIP newsprint and bag paper. This vibration mode occurs always at the roll rotation frequency and is hence not accompanied with audible sound. On a two-drum winder the rolls are seen to bounce in a more or less irregular pattern from drum to drum. Due to the roll eccentricity, also the core chucks are vibrating heavily. The mechanism and mode for this type of vibration is quite complex, involving interplay of the adjacent rolls due to the edge contact and frictional forces.

c) Wound roll excited drum resonance vibration

This vibration occurs generally at steady running speed when a multiple of the wound roll rotation frequency matches or is in the vicinity of the drum natural frequency. Depending on the running speed and the value of the natural frequency, the multiple number of the rotation frequency can be 2, 3, 4 or 5. Paper grades vibrating in this mode include uncoated fine paper and sackkraft.

Common for all these above mentioned vibration categories is that they are generated by an oscillating nip load which is synchronous to the wound roll rotation frequency or its multiple. Although a large part of the nip induced roll deformation recovers in one revolution of the roll, some residual deformation is fed back during the reentry into the nip. This results in a self-enforcing vibration state, where the roll surface deformations and nip load oscillations grow hand in hand.

One of the earliest papers where the essential features of this self-excited vibration mechanism were explained was written by Daly [1]. Without any modeling, Daly explained the vibration phenomena using a washboard road analogy. Later Möhle *et al.* [2] studied two-drum winder vibrations and developed a simple one-degree-of-freedom mathematical model based on experimental observations. In their model, the generation of the wavy roll was implemented as a purely plastic residual deformation developed one revolution earlier and reentering the nip. Although the model was simple, they could nicely explain the unstable regions occurring at certain roll rotation frequencies. A more comprehensive two-drum winder model including all interacting structural elements of the wind up was presented by Jorkama [3]. Various eigenmodes of the wind up were presented and requirements for damping the vibrations were studied. However, the self-enforcing development of the wavy roll surface was omitted. Sueoka *et al.* [4] have presented an analogous calender rubber roll-covering polygonalization model. In their model, the development of the roll surface deformation pattern is based on a viscoelastic model of the behavior of the rubber cover. Their model results in a constant coefficient, linear, time delay ordinary differential equation system which stability is extensively studied.

The present paper follows the outline of Ref. [4]. In addition, some characteristic features of winding, such as the time dependence of the coefficients of the differential equations and rotation frequency of the wound roll, are included. The authors believe that even this simple model can elucidate the essential features of the winder vibrations and, hence, lead the way to reduce the costly problems due to winder vibrations.

THEORY

Consider the wind up model of Figure 1 consisting of the winding drum, depicted as the lower uniform circle, and the wound roll, depicted as the wavy upper circle. On the right, the wind up is in its undeformed state and on the left in its deformed state. The winding drum cover is undeformable but has a translational vertical degree of freedom x_1. The deviation of the wound roll's shape from circular is denoted by $e(t)$. In addition, the wound roll has a vertical translational degree-of-freedom, denoted by x_2.

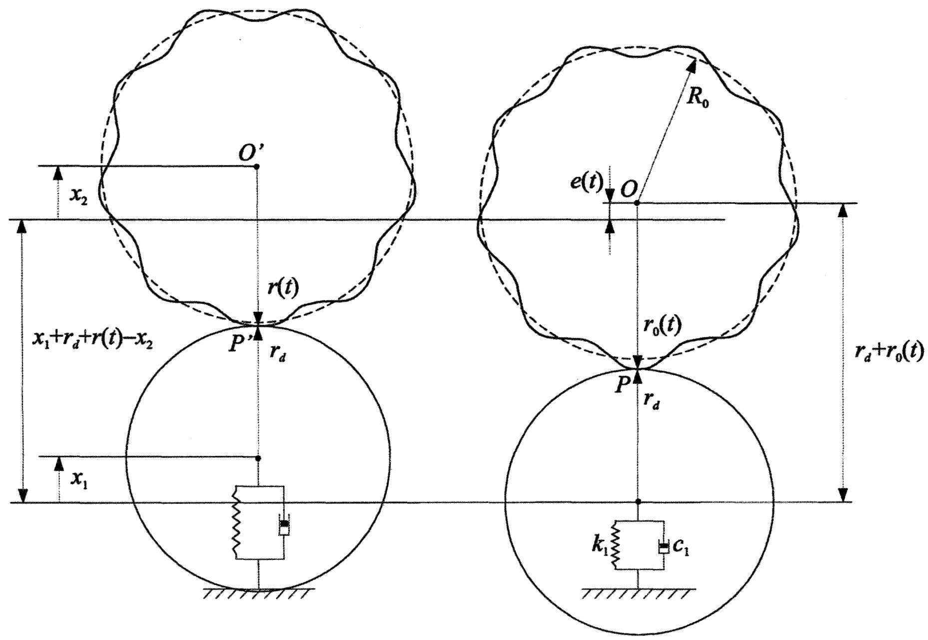

Figure 1. Deformed (left) and undeformed (right) configurations.

From Figure 1 we see the following geometrical relation

$$x_1 + r(t) - x_2 + e(t) = r_0(t) \; . \qquad (1)$$

Denoting the nip compression by δ, the deformed radius $r(t)$ can be represented as

$$r(t) = r_0(t) - \delta \; , \qquad (2)$$

Substituting (2) to (1) yields

$$x_1 - x_2 + e(t) = \delta. \qquad (3)$$

This compression occurs between the points O and P. In this simple model, the description of the response of δ to the nip loading constitute the *constitutive equation* of the winding roll and, hence, will determine dominantly the system

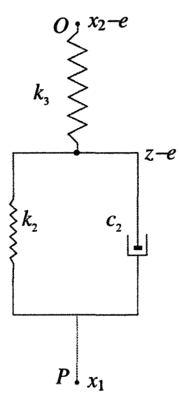

Figure 2. Description of the paper roll deformation element.

characteristics. In general, this equation should be formulated so that it reflects the observed deformation characteristics of the paper roll as close as possible. With a high number of internal degrees of freedom, the behavior can be described accurately but the understanding and interpretation of the model predictions become more difficult. In this paper, the emphasis lies in the ease of the interpretation of the qualitative behavior. Hence, a viscoelastic constitutive model with only one internal degree of freedom (three independent parameters) is chosen for describing the deformation characteristics of the wound roll.

The equations of motion become

$$\begin{aligned} &m_1\ddot{x}_1 + k_1 x_1 + c_1\dot{x}_1 + k_2\left[x_1 - z + e(t)\right] + c_2\left[\dot{x}_1 - \dot{z} + \dot{e}(t)\right] = 0\ , \\ &k_2\left[x_1 - z + e(t)\right] + c_2\left[\dot{x}_1 - \dot{z} + \dot{e}(t)\right] + k_3\left(x_2 - z\right) = 0\ , \\ &m_2\ddot{x}_2 + k_3\left(x_2 - z\right) = 0\ . \end{aligned} \tag{4}$$

Apparently $e(t)$ is a function (or functional) of the nip deformation occurred one revolution earlier. Denoting by $u(t)$ the nip deformation and by T the revolution period, this relation reads

$$e(t) = F(u(t-T)). \tag{5}$$

The nip-induced deformation of the spring element k_3 is instantaneously recovered, whereas the deformation of the element c_2-k_2 is restored only partially during one revolution. The deformation of this element, which is denoted by u, is

$$u = x_1 - z\ , \tag{6}$$

where the sign of u is chosen so that compression is positive. After exiting the nip, this element is free, and hence, the balance equation reads

$$k_2\tilde{e} + c_2\dot{\tilde{e}} = 0\ , \tag{7}$$

where $\tilde{e}$ denotes the position of this element in the course of one revolution. The solution of equation (7) is

$$\tilde{e}(t) = -u(t_1)e^{-\alpha(t-t_1)}\ , \tag{8}$$

where

$$\alpha = \frac{k_2}{c_2} \tag{9}$$

and t_1 the time when the circumferential location under consideration passed the nip last time. Since $e(t)$ is defined as the deviation of the wound roll from circular shape just before entering the nip, the expression

$$e(t) = -u(t-T)e^{-\alpha T} \tag{10}$$

is obtained. Inserting the result (10) to the equations of motion (4) gives

$$\begin{aligned} &m_1\ddot{x}_1 + c_1\dot{x}_1 + k_1x_1 + k_2w + c_2\dot{w} = 0 , \\ &k_2w + c_2\dot{w} + k_3\left(x_2 - z\right) = 0 , \\ &m_2\ddot{x}_2 + k_3\left(x_2 - z\right) = 0 , \end{aligned} \tag{11}$$

where

$$w(t) = u(t) - e^{-\alpha T}u(t-T) . \tag{12}$$

Rearranging Eqs. (11) gives

$$\begin{aligned} &m_1\ddot{x}_1 + c_1\dot{x}_1 + (k_1 + k_3)x_1 - k_3(x_1 - z) - k_3x_2 = 0 , \\ &k_2w + c_2\dot{w} - k_3x_1 + k_3\left(x_1 - z\right) + k_3x_2 = 0 , \\ &m_2\ddot{x}_2 + k_3x_2 - k_3x_1 + k_3\left(x_1 - z\right) = 0 . \end{aligned} \tag{13}$$

It should be noted that in the analysis α is taken as an independent parameter since with the current constitutive model it is not possible to describe simultaneously the nip damping and the dent recovery on the roll surface.

In order to analyze the stability of the system, the Laplace transformation is performed for Eq. (13). The revolution period T is treated as a constant when the Laplace transformation is done. During most of the winding cycle, this is a good assumption since the angular frequency of the roll does not change much during one roll revolution. When all initial values are set to zero, the Laplace transformation yields

$$\mathbf{AX} = \mathbf{0} \tag{14}$$

where

$$\begin{aligned} &\mathbf{X} = (X_1, X_1 - Z, X_2)^t , \\ &\mathbf{0} = (0,0,0)^t \end{aligned} \tag{15}$$

and

$$\mathbf{A} = \begin{bmatrix} g_1 & -k_3 & -k_3 \\ -k_3 & g_2 & k_3 \\ -k_3 & k_3 & g_3 \end{bmatrix} , \tag{16}$$

where

$$g_1 = m_1 s^2 + c_1 s + k_1 + k_3 \ ,$$
$$g_2 = k_3 + (c_2 s + k_2)\left[1 - e^{-(\alpha+s)T}\right] \ , \tag{17}$$
$$g_3 = m_2 s^2 + k_3 \ .$$

RESULTS

Characteristic of winder dynamics is that both the excitation and natural frequencies change with time. The change of the excitation frequency stems from the constantly increasing roll diameter and changing running speed, which consists of acceleration, steady running speed and deceleration. The natural frequencies change because the mass of the paper roll increases during winding. According to experimental winder vibration studies [3], it is known that in severe vibration cases the excitation source is almost exclusively the wound roll. Hence, it is instructive to start with determining the situations when the multiples of the roll rotation frequency hit the resonances. Figure 3 depicts the natural frequency curves (solid lines) together with the first and second harmonics of the roll rotation frequency (dashed lines) during one winding cycle. The model parameters are chosen to be representative for a modern wide winder running newsprint grade. These parameters are shown in Table 1. The drum stiffness is determined from a modal measurement and the roll spring constant from a roll compression test. The recovery coefficient α is most accurately measured from the paper roll by indenting it with some "bump" attached onto the winding drum surface and observing the recovery of the dent caused by the indenter. Here, however, a much simpler test set up was used to obtain an estimate for α. A relaxation test was performed for a pile of newsprint (height 4 cm, area 7 cm x 7 cm). Initially 1 MPa pressure was applied and then the compression was kept constant and the decay in the pressure was observed. The data was fitted into a six parameter linear, viscoelastic model. The calculated relaxation time constants corresponded to the following values of α: 0.35, 0.033 and 0.0033 1/s.

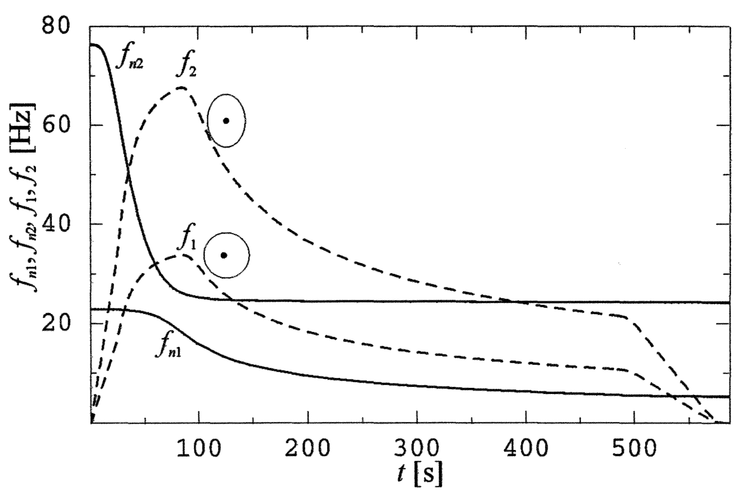

Figure 3. Natural frequencies of the system f_{n1} and f_{n2} (solid lines), the roll rotation frequency f_1 (lower dashed line) and the second harmonic of the roll rotation frequency f_2 (upper dashed line) as a function of time t.

Table 1.

Parameter values used in the calculations

Parameter	Notation	Value
Paper thickness	τ	63 μm
Acceleration	a	0.5 m/s^2
Deceleration	b	0.5 m/s^2
Steady state running speed	v_0	40 m/s
Rounding time in the running speed	t_p	12 s
Core diameter	d_0	0.1 m
Final roll diameter	d_e	1.25 m
Paper density	ρ	750 kg/m^3
Winding drum mass	m_1	4000 kg
Winding drum stiffness	k_1	83.5 MN/m
Winding drum damping	c_1	7 kNs/m
Mass of the core/length	m_0	5 kg/m
Stiffness coefficient of the viscoelement	k_2	100 MN/m
Damping coefficient of the viscoelement	c_2	10 kNs/m
Stiffness coefficient of the roll	k_3	10 MN/m
Recovery coefficient	α	0.1 1/s

During the first 50 seconds, the shapes of the eigenmodes corresponding these natural frequencies are well localized. Within this time region, the first eigenmode consists of high amplitude movement of the drum and negligible movement of the roll whereas in the second mode the opposite movements occur.

In the interval 50 –120 s, when the natural frequencies are closest to each other, the modes are such that the amplitudes of the winding drum and the roll are comparable. In the first eigenmode, the winding drum and the roll move in the same phase and in the second mode in opposite phases.

During the rest of the winding cycle, after 120 s, the modes become again localized. The first eigenmode is the wound roll mode and the second one the winding drum mode.

It can be seen from Figure 3, that the first natural frequency f_{n1} becomes equal to the first or second roll harmonic only during the acceleration ($t \approx$ 20s and 40 s) and deceleration ($t \approx$ 530 s and 560 s). During the steady running speed, the roll rotation frequency at this running speed is always higher than f_{n1}.

The second natural frequency f_{n2} becomes first equal to the second roll harmonic at approximately 40 s and shortly later equal to the first roll harmonic. Both these incidents occur during the acceleration. Later, at $t \approx$ 400 s, during the steady running speed phase, the second roll harmonic becomes again equal to the second natural frequency.

From Eq. (14), the characteristic equation is given by

$$\det \mathbf{A} = 0 . \tag{18}$$

Since there exists a time lag, there are an infinite number of characteristic roots s_i of Eq. (18). The system is stable if all the real parts of these roots are negative. On the other hand, the system is unstable if one or more real parts are positive.

The evolution of the first and second characteristic roots during the winding cycle are shown in Figs. 4 and 5, respectively. The upper panel shows the imaginary part together with the second natural frequency and the lower panel the real part. The imaginary part of s_1 follows most of the time the f_1-curve. At the end of the acceleration stage and at the beginning of the steady running speed stage, it coincides with the second natural frequency f_{n2}. At this location, there exists a wide unstability region. Although the vibration frequency here is lower than generally in the vibration case a), for this single drum winder model this corresponds to the vibration during the initial acceleration.

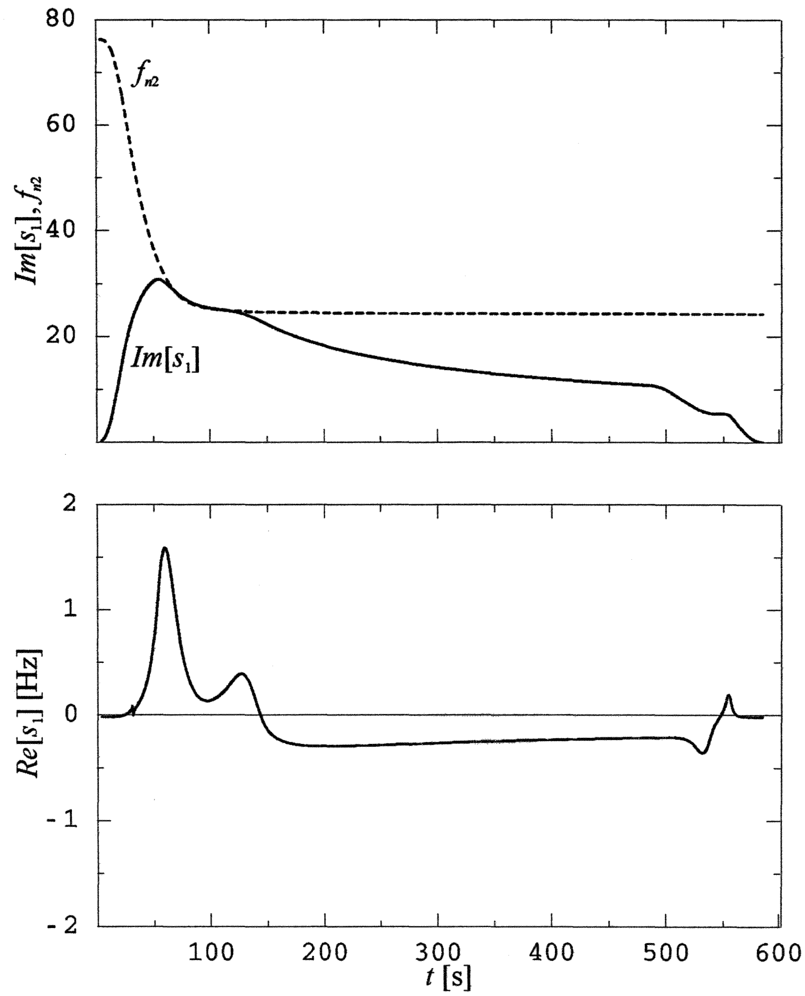

Figure 4. The imaginary (upper panel) and real (lower panel) parts of the first characteristic root.

The imaginary part of the second characteristic root in Fig. 5 follows during the acceleration and deceleration the second harmonic of the roll and during most of the steady running speed stage the second natural frequency. There are short duration unstability regions during the acceleration and deceleration stages and a longer region between 350 s and 430 s. This latter region can be related to vibration category c) since the second harmonic of the roll excites the natural frequency of the winding drum.

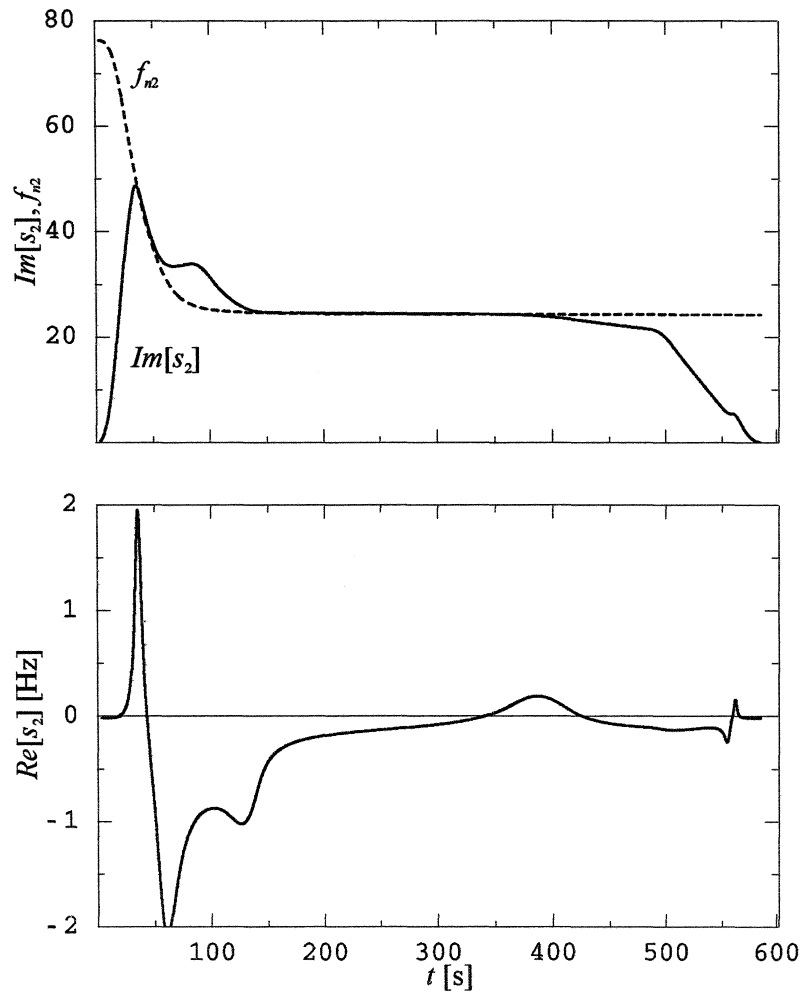

Figure 5. The imaginary (upper panel) and real (lower panel) parts of the second characteristic root.

A parameter study revealed that for values of α larger than 50 1/s, the system is always stable and for values of α smaller than 0.1 1/s the system becomes quite immune for any changes of α. In the viscoelastic measurement of paper, the relative weighting of the estimated α's should also be taken into account. The smaller the weighting of the small values of α is, the stabler the material is.

In this model, the winding drum stiffness does not seem to have any other influence than slightly shifting the unstability zones. Increasing the winding drum damping is beneficial, since it shrinks the unstability regions of all characteristic roots. However, it is not very effective, since doubling, which might be very difficult to accomplish in practice, of the damping produced only approximately 10 – 20 % shorter unstability regions. Doubling of the roll damping didn't have practically any influence on the stability. This is because the first natural frequency (which activates the roll damping) is excited only during the acceleration and deceleration for short periods. For a two-drum winder, the case would be different since the natural frequencies related to the wound roll movement are higher due to the additional front drum and rider roll nips.

CONCLUSIONS

With the present model, the most common winder vibration cases could be represented. Due to the time lag in the system equations, negative damping is fed into the system and during certain stages along the winding cycle the system becomes unstable. In the studied example, long, unstable zones were found at the end of the acceleration stage and later at steady running speed when the second harmonic of the roll matched the second natural frequency. These unstability zones were identified as "vibration during the initial acceleration" and "wound roll excited drum resonance vibration" which are well known in practice. The non-existence of the third common winder vibration case "roll bouncing" in single drum winders was explained by studying the excitation and natural frequencies.

The are several directions how to further develop the model and analysis. One possibility is to model the winder structure more accurately and extend it to two-drum winding. Another, maybe more challenging possibility, is to improve the constitutive description of the wound roll.

REFERENCES

1. Daly, D., 'How paper rolls on a winder generate vibration and bouncing'. Paper Trade Journal **151**, pp. 48-51 (1967).
2. Möhle, H., Buschmann, G. and Müller, G., 'Vibration an Papierrollmaschinen', Das Papier **11**, pp. 845-850 (1970).
3. Jorkama, M., 'On the winder vibration analysis', Licentiate's thesis Helsinki University of Technology, 1996.
4. Sueoka, A., Ryu, T., Kondou, T., Tsuda, Y., Katayama, K., Takasaki, K., Yamaguchi, M., Hirooka, H., 'Polygonal deformation of roll-covering rubber,' JSME International Journal, Series C, **39**(1), pp. 1-10, 1996.